Indian Journal of Engineering & Materials Sciences
Vol. 29, October 2022, pp. 686-695
DOI: 10.56042/ijems.v29i5.48673

Influence of Process Parameters on Mechanical and Microstructural Property of Dissimilar Friction Stir Welded Joints of Armor Aluminium Alloys AA7039 and AA5083

Gyander Ghangas[a,b,*], & Sandeep Singhal[b]

[a]Department of Mechanical Engineering, SRMIST, NCR Campus, Ghaziabad, Uttar Pradesh 201 204, India

[b]Department of Mechanical Engineering, National Institute of Technology, Kurukshetra, Haryana 136 119, India

Received: 9 April 2021; Accepted: 21 September 2021

Friction stir welding (FSW) is an innovative, green and energy-efficient solid-state welding process. Which has been resolved the problems of defects related to microstructure and mechanical properties of welding joints of soft materials. FSW is also capable to join dissimilar materials of different melting points together with adequate efficiency and effectiveness. Present research work is an attempt to join the two dissimilar armor grad aluminium alloys i.e. AA7039 and AA5083 by FSW. Both materials are utilized as armor materials in defence. The process parameters such as tool rotation speed (RS), welding speed (WS) and tool tilt angle (TA) were utilized for variation at different five levels for experimentation. The experiments were designed by center composite design (CCD) of response surface methodology (RSM). The fabricated joints were examined for the variation in mechanical properties such as ultimate tensile strength (UTS), yield tensile strength (YTS) and percentage elongation (EL). Effects of the inputs parameters on the variation of the responses were validated by analysis of variance (ANOVA). The obtained results of aforesaid properties were utilized for the optimization of input parameters in the desirability approach. The desirability approach revealed that 1440 RPM of tool rotation, 32.1 welding speed and 2.4 tilt angle as an optimized set of parameters, which can fabricate the joint with 263.02 MPa UTS, 211.90 MPa YTS and 14.7% EL. The results of ANOVA and optimization were also verified by a change in the microstructure of FSWed joints.

Keywords: Dissimilar Friction Stir Welding, Defence Materials, Parameters Optimization, Microstructure, ANOVA

1 Introduction

Friction Stir Welding (FSW) process is invented and patented by W. M Thomas at The Welding Institute (TWI) in 1991[1]. FSW is a joining process that utilizes frictional heat and mechanical stiring to produce a high-quality joint. In this process, a non-consumable tool is used. The tool emerges a shoulder for the generation of frictional heat and a profiled pin for mechanical stiring action[2]. The joining of materials without melting i.e. in solid-state make it a versatile process that make it able to join different materials and alloys including Al, Ti, Mg, steel, copper and metal matrix composites in similar and dissimilar condition[3,4]. It also has been provided the opportunity to the manufacturers in aerospace, defense, automobile, railways and many other industries that they can use dissimilar aluminium alloys for fabrication. Because it overcomes the problems of welding of dissimilar alloys due to differences in their metallurgical, mechanical, thermal and chemical properties[5,6].

Welding of dissimilar metals and alloys using FSW has gained momentum among researchers in the recent few years. Many useful and interesting results have been extorted on mechanical properties and thermal history of dissimilar FSW joints[7]. The results and of the previous studies are presented in Table 1.

Other aluminium alloys such as AA2219-AA7039[23], AA6082 – AA7075[24], AA6061 – AA7050[25], AA6082 – AA 2024[26], AA2024 – AA7075[27] and AA2019 – AA5083[28] and many more are also successfully welded and reported in the previous literature. But to the author's knowledge, the aluminium alloys AA7039 and AA5083 are not reported by any researcher in the literature. There is also the scarcity of the work for multi-objective process parameter optimization for FSW of dissimilar metals.

The above said alloys of aluminium are medium strength alloys, which have good ballistic characteristics.

*Corresponding author (E-mail: ghangas01@gmail.com)

Table 1 — Literature Review for dissimilar FSW

S. No	Authors/year	Work Material	Objective/Process Parameters	Investigated Responses	Findings
1	S.W. Park *et al.*[8] (2017)	AA 6111/ AA5023	Shoulder Diameter (SD), Weld Pitch (WP), Rotating Speed and welding speed	Tensile Fracture peak Load	Higher the SD and WP produced higher peak load, peak load decreased inversely in case of the higher rotation speed[8].
2	R.S.S Prasnth and K. Hans Raj[9] (2017)	AA6251/ AA6061	Rotational speed, Traverse speed, Axial force	Ultimate strength (US), Yield strength (YS), % elongation (%EL)	US and % EL were found maximum at 600 RPM, 60 mm/min and 6KN, rotation speed, traverse speed and axial force respectively. YS was maximum at 600 RPM rotational speed, 30 mm/min welding speed and 9 KN axial force[9].
3	Avinash P *et al.*[10] (2013)	AA 2023 T3/ AA 7075 T6	To check the feasibility FSW for plate thickness ratio more than 1.3/ rotating speed and transverse speed	Microstructure and mechanical properties	Medium rotating speed (1000 RPM) and lower transverse speed (80 mm/min) found efficient welding parameters, highly refined grains in the nugget zone due to less frictional heat[10].
4	Ravikumar S, *et al.*[11] (2013)	AA7075 T651/AA 6061 T651	Rotational speed, transverse speed and pin profiles	Mechanical strength and microstructure	Maximum tensile strength (205.23 MPa) achieved at 90 mm/min welding speed, 900 RPM rotational speed and with taper cylindrical pin profile[11].
5	Yuhua Chen *et al.*[12] (2018)	Ti6Al4V/ AA2024	Fixed rotating sped and welding speed, threaded cylindrical pin	Mechanical strength, microstructure	83% ultimate tensile strength, fail with ductile-brittle fracture mode. Stir zone was a mixture of recrystallized grains of Aluminium-Titanium particles[12].
6	Hossein Karami Pabandi *et al.*[13] (2018)	AA2024-T6/AA6061-T6	position of alloys, effects of precipitation hardening, heat treatment in retreating and advancing side	Micro hardness, tensile strength and microstructure	After heat treatment grain coarsening appears in microstructural analysis, tensile strength was found more when 6061 was on the advancing side[13].
7	Chenghang Zhang *et al.*[14] (2020)	AA2014/ AA7075	Welding Speed	Shear texture, grain size	Shear texture increased with a decrease in welding speed and grain size of NZ increased with an increase in the same[14].
8	Mohamed Mohamed Zaky Ahmed *et al.*[15] (2021)	AA5083/ AA5754	Tool rotational speed and welding speed	Average grain size of NZ	A decrease in rotational speed caused a reduction in the grain size of NZ. But it was also revealed that welding speed has no significant effect on the change in grain size of NZ[15].
9	Mohamed M. Z. Ahmed *et al.*[16] (2021)	AA2024/ AISI1018	Tool rotational speed and welding speed	Microstructure and mechanical properties	Higher welding speed or lower rotational speed can fabricate the joints with maximum tensile strength and higher elongation. Lower welding speed caused the high heat input which results in a continuous layer of AL rich IMCs in NZ[16].
10	M. Ilangovan *et al.*[17] (2015)	AA6061/ AA5086	Tool rotational speed, Tool traverse speed, Axial force	microstructural features and tensile properties.	maximum hardness of HV 115 and a joint efficiency of 56%[17],
11	R B Iyer *et al.*[18] (2016)	AA6061/ AA6082	Spindle speed and welding speed	Tensile strength, microhardness and microstructure	The maximum tensile strength (66.06 MPa) and 92 HV hardness was observed without Cu powder. With Cu powder at 1400 RPM and 20 mm/min welding speed, these were observed as 96.54 MPa and 105 HV respectively[18].
12	Jitender Kundu, Hari Singh[19] (2016)	AA5083/ AA5086	welding speed, pin profiles, tilt angle	tensile strength, percentage of elongation	Optimum parameter setting for UTS and %age elongation were 1000 RPM, 2° tool tilt angle[19].
13	Sumit Jain, *et al.*[20] (2017)	AA6082/ AA5083	tool rotation speed, welding speed, tool pin profile, shoulder diameter	Elongation, ultimate tensile strength	Optimum parameters setting for UTS and elongation was found 1200 RPM rotational speed, 30 mm/min welding speed, trapezoidal pin profile and 14 mm tool shoulder diameter[20].
14	E. T. Akinlabi *et al.*[21] (2017)	AA5754/ C11000	Tool rotation speed and transverse speed	Residual stresses	The compressive residual stresses were observed in most of the joints. But the joint weld with 950 RPM and 150 mm/min welding speed showed tensile stresses[21].
15	Xun Liu *et al.*[22] (2014)	AA 6061/ TRIP780/ 800 steel	Tool rotation speed, welding speed and tool offset	Tensile strength, microstructure	Weld nugget was seemed as aluminum matrix composite, maximum tensile strength was achieved as 82% of AA 6061[22].

These two alloys are primarily used in defense vehicles as armor materials. Both alloys have common applications such as in defense, automobile, railways and in the structure fabrication industry. So there always be required to be joined at several places to use these two together. Therefore AA 7039 and AA 5083 are selected as the base materials for this study.

The main objectives of the present study are to ascertain the effect of process parameters of FSW on the properties of joints and also determine the optimum set of parameters of FSW process for the dissimilar welding of these alloys.

2 Materials and Method

In the present experimental examination, aluminium alloys AA 7039 T6 and AA 5083 T651 are utilized as the base materials with 5 mm thickness. The chemical composition and mechanical properties are presented in Table 2 and Table 3 respectively. The work material utilized in this research work is cut in two 75 mm X 150 mm dimensions to prepare a 150 mm X 150 mm but weld joint. These pieces are welded on a 4 HP, Vertical Milling machine featured with a specially designed fixture at central workshop of National Institute of Technology, Kurukshetra, India (Fig. 1 (a). The tool made of H13 tool steel contains 18 mm shoulder with 2 mm shoulder flatness and square pin profile with 6 mm diameter and 4.8 mm height is used for FSW as presented in Fig 1 (b).

All the welded joints were tested for tensile properties such as Ultimate Tensile Strength (UTS), Yield Tensile Strength (YTS) and Percentage Elongation (EL). Tensile test specimens are prepared according to ASTM E 08M specifications. For experimentation three process parameters are considered at their five different levels, these parameters and levels are shown in Table 4. Experiments are designed by center composite design (CCD) of response surface methodology (RSM). The suggested set of parameters for experimentation by the aforesaid technique is presented in Table 5 with the results of tensile properties.

Table 2 — Chemical properties of AA7039 and AA5083

Elements	Zn	Mg	Mn	Fe	Si	Cu	Cr	Al
AA7039	4.521	1.082	0.462	0.3	0.267	0.038	0.0192	Remaining
AA5083	0.03	4.3	0.63	0.13	0.076	0.005	0.06	Remaining

Table 3 — Mechanical properties of AA 7039 and AA5083

	Tensile Strength	Yield Strength	% Elongation	Vickers Hardness
7039	414Mpa	328Mpa	15.1	135 VHN
5083	317	228	16	96

3 Results and Discussion:

Analysis of variance (ANOVA) was performed to check the adequacy of developed models for all three responses. ANOVA results are presented in Table 6, Table 7 and Table 8 for UTS, YTS and EL, respectively.

The above-presented tables reveals that the developed models are significant with the F- values of 205.12, 150.03 and 14.43 for UTS, YTS and EL, respectively. Less than 0.050 value of "Prob>F" is the indication of the significance of model terms. In the present study RS, WS, TA, RS x WS, WS x TA, RS x TA, RS^2, WS^2 and TA^2 are significant individual, interactional and square terms for UTS model.

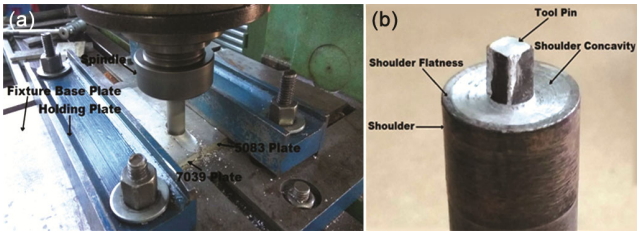

Fig 1 — Experimental setup and tool design.

Table 4 — Process parameters and levels

Process Parameters	Units	Range				
		-2	-1	0	1	2
Rotational Speed (RS)	rpm	792	1000	1500	2000	2207
Transverse Speed (WS)	mm/min	24	30	45	60	66
Tilt Angle (TA)	Degree	1	1.5	2.5	3.5	4

Table 5 — Design of experiments suggested by RSM

Experiment No.	Rotating Speed (rpm)	Welding Speed (mm/min)	Tilt Angle (degree)	UTS (MPa)	YTS (MPa)	EL (%)
1	2000	60	1.5	148	125	8.8
2	2000	30	3.5	221	170	10.9
3	1000	60	3.5	158	150	8.9
4	1000	30	1.5	210	157	13.4
5	792	45	2.5	155	128	7.6
6	2207	45	2.5	245	198	11.6
7	1500	24	2.5	258	208	14.5
8	1500	66	2.5	190	140	10.5
9	1500	45	1.0	181	140	09.8
10	1500	45	4.0	241	187	14.0
11	1500	45	2.5	260	200	13.9
12	1500	45	2.5	262	203	14.6
13	1500	45	2.5	255	206	13.9
14	1500	45	2.5	254	210	13.7
15	1500	45	2.5	256	205	13.8
16	1500	45	2.5	255	203	12.1

Table 6 — ANOVA results for UTS

Source	Sum of Squares	df	Mean Square	F Value	p-value Prob> F	
Model	26412.59	9	2934.73	205.12	< 0.0001	significant
A-RS	4050	1	4050	283.07	< 0.0001	
B-WS	2312	1	2312	161.59	< 0.0001	
C-TA	1800	1	1800	125.81	< 0.0001	
AB	509.64	1	509.64	35.62	0.0010	
AC	103.92	1	103.92	7.26	0.0358	
BC	1993.30	1	1993.30	139.32	< 0.0001	
A2	7050.78	1	7050.78	492.81	< 0.0001	
B2	2502.78	1	2502.78	174.93	< 0.0001	
C2	4680.28	1	4680.28	327.12	< 0.0001	
Residual	85.84	6	14.30			
Lack of Fit	33.84	1	33.84	3.25	0.1311	not significant
Pure Error	52	5	10.4			
Cor Total	26498.44	15				
Std. Dev.	3.78		R-Squared		0.996	
Mean	221.81		Adj R-Squared		0.991	
C.V. %	1.70		Pred R-Squared		0.860	
PRESS	3686.01		Adeq Precision		36.053	

Table 7 — ANOVA results for YTS

Source	Sum of Squares	df	Mean Square	F Value	p-value Prob> F	
Model	15050.88	9	1672.32	150.04	< 0.0001	significant
A-RS	2450	1	2450	219.81	< 0.0001	
B-WS	2312	1	2312	207.43	< 0.0001	
C-TA	1104.5	1	1104.5	99.095	< 0.0001	
AB	101.30	1	101.30	9.088	0.0236	
AC	243.83	1	243.83	21.87	0.0034	
BC	1539.98	1	1539.98	138.16	< 0.0001	
A^2	3240.12	1	3240.12	290.70	< 0.0001	
B^2	1711.12	1	1711.12	153.52	< 0.0001	
C^2	3160.12	1	3160.12	283.52	< 0.0001	
Residual	66.87	6	11.14			
Lack of Fit	9.37	1	9.375	0.815	0.4080	not significant
Pure Error	57.5	5	11.5			
Cor Total	15117.75	15				
Std. Dev.	3.33		R-Squared		0.995	
Mean	176.87		Adj R-Squared		0.988	
C.V. %	1.88		Pred R-Squared		0.928	
PRESS	1081.59		Adeq Precision		32.15	

Table 8 — ANOVA results for EL

Source	Sum of Squares	df	Mean Square	F Value	p-value Prob> F	
Model	73.92	7	10.56	14.43	0.0006	significant
A-RS	8	1	8	10.93	0.0107	
B-WS	18.53	1	18.53	25.34	0.0010	
C-TA	8.52	1	8.52	11.65	0.0092	
AB	8.55	1	8.55	11.68	0.0091	
BC	8.50	1	8.501	11.62	0.0092	
A^2	30.42	1	30.42	41.58	0.0002	
C^2	5.28	1	5.28	7.22	0.0276	
Residual	5.85	8	0.73			
Lack of Fit	2.26	3	0.75	1.05	0.4478	not significant
Pure Error	3.59	5	0.72			
Cor Total	79.77	15				
Std. Dev.	0.855		R-Squared		0.926	
Mean	12.048		Adj R-Squared		0.862	
C.V. %	7.098		Pred R-Squared		0.804	
PRESS	15.619		Adeq Precision		13.315	

Similarly, RS, WS, TA, RS x WS, RS x TA, WS x TA, RS^2, WS^2 and TA^2 for YTS and RS, WS, TA, RS x WS, WS x TA, RS^2 and TA^2 for EL are found significant model terms. The model terms that have "Prob>F" value greater than 0.05 are non-significant terms and are removed by backward elimination. Lack of fit in the model has "Prob>F" values 0.131, 0.408 and 0.447 for UTS, YTS and EL, respectively implies that the lack of fit is not significant compared to the pure error. The integrity of the model is checked by the value of the coefficient of determination "R^2" and it should be close to 1 for the righteousness of the model. The value of "R^2" is 0.996, 0.995 and 0.926 for the model of UTS, YTS and EL, respectively. This implies that 99.6%, 99.5% and 92.6% experimental data confirm the compatibility with the predicted data of the developed models for UTS, YTS and EL respectively. The values of predicted R^2 and adjusted R^2 are 0.860 and 0.991 for UTS; 0.928 and 0.988 for YTS; and 0.804 and 0.862 for EL, which shows the reasonable agreement between these two. Signal to noise ratio is measured by adequate precision and it is desired to be greater than 4. The adequacy of the signals is indicated by obtained values of adequate precision which is 36.0, 32.1 and 13.3 for UTS, YTS and EL models, respectively. The predicted and observed values are scattered close to the 45^o line, which indicates a nearly perfect fit of all three developed experimental models. The falling of the residuals on a straight line for all three developed models confirms the normal distribution of the errors. To verify the mathematical models confirmatory tests were conducted using values of process parameters other than those used in the suggested design matrix[29-31].

In the present study, the response under consideration are UTS, YTS and EL, which are the functions of the considered input parameters (RS, WS and TA). This function can be expressed as:

$$Y = f(RS, WS, TA) \quad \ldots (1)$$

Where Y is the output of the process and RS, WS and TA are the tool rotational speed; welding speed and tool tilt angle i.e. process input parameters.

The DESIGN EXPERT software was used to calculate the coefficients of regression analysis for different responses. Mathematical models were developed with these calculated coefficients, which are presented in coded form in the Equations (2), (3) and (4) for UTS, YTS and EL, respectively.

$$UTS = 257.593 + 31.819 \times A - 24.041 \times B + 21.213 \times C + 15.963 \times A \times B + 7.208 \times A \times C + 31.569 \times B \times C - 29.687 \times A^2 - 17.687 \times B^2 - 24.187 \times C^2 \quad \ldots (2)$$

$$YS = 204.187 + 24.748 \times A - 24.041 \times B + 16.617 \times C + 7.117 \times A \times B - 11.0416 \times A \times C + 27.748 \times B \times C - 20.125 \times A^2 - 14.625 \times B^2 - 19.875 \times C^2 \quad \ldots (3)$$

$$EL = +13.43 + 1.41 \times A - 1.522 \times B + 1.460 \times C + 2.0676 \times A \times B + 2.0617 \times B * C - 1.95 \times A^2 - 0.8125 \times C^2 \quad \ldots (4)$$

3.1 Adequacy of developed model

The experiment was performed to confirm the adequacy of the developed mathematical models for each response. The combination of levels of process parameters other than that in the DOE matrix was chosen for the confirmatory test. The results of the test are presented in Table 9 which clearly shows that the developed models are adequate to predict the responses. Where, error observed in acceptable limits as 4.1%, 2.2% and 6.3% for UTS, YTS and EL respectively.

3.2 Effect of process parameters on UTS

As presented in the results of ANOVA all three considered parameters are found to significantly contributed to the variation of the considered responses i.e. UTS, YTS and EL of dissimilar FSWed joints of AA7039 and AA5083. The variation of these responses with the variation of the process parameters is presented in Fig 2 (a) by perturbation curves. These curves reveal that UTS is increased when RS is increased up to 1850 RPM and then start decreasing on further increment in the same. The increase in the WS from minimum (24 mm/min) up to 30 mm/min caused the increase in the UTS but more increment in WS makes the UTS decreased. The increment in the UTS can be seen until TA increases up to 3.5^o and then starts decreasing with further increment in the same.

As discussed earlier, that the change in the RS causes the change in the heat generation due to more

Table 9 — Results of the confirmatory test

Result condition	RS (RPM)	WS (mm/min)	TA (Degree)	UTS (MPa)	YTS (MPa)	EL (%)
Predicted	1550.66	31.89	2.56	266.19	215.06	14.67
Observed	1550.66	31.89	2.56	255.6	220.1	13.8
Error (%)	----	---	----	4.1	2.2	6.3

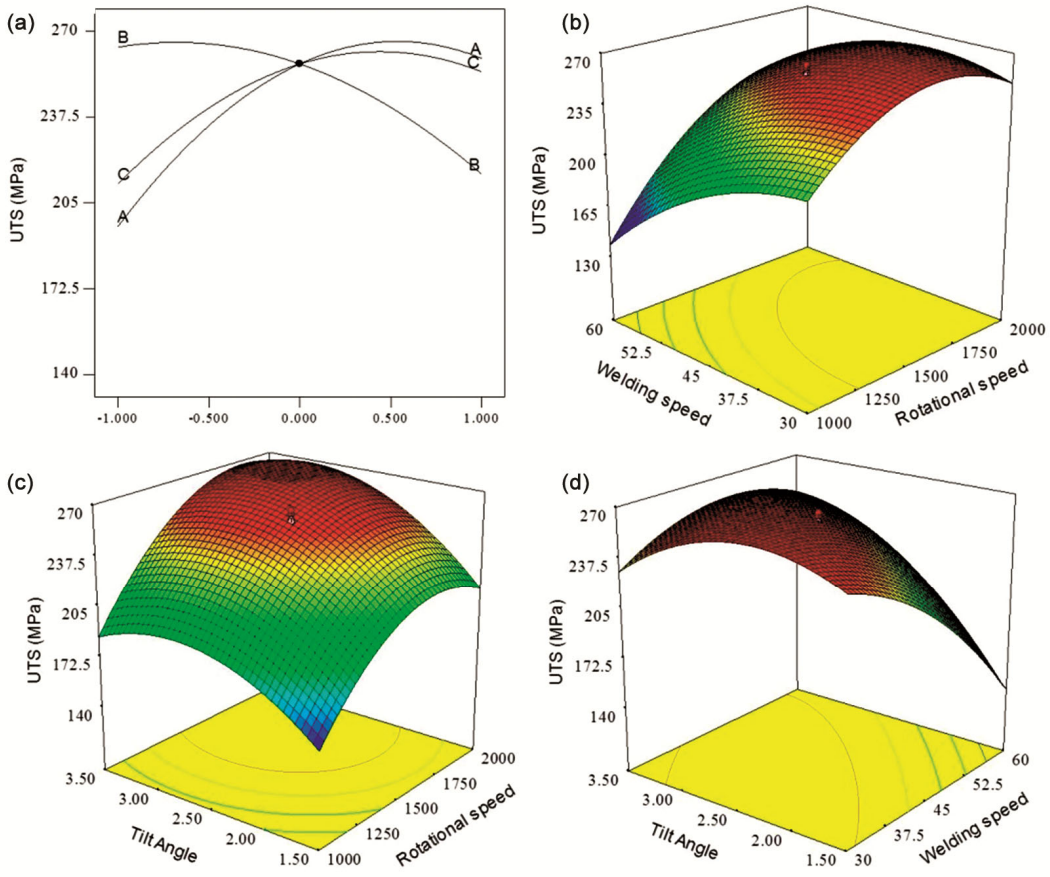

Fig. 2 — ANOVA plots for main and interactional effects of process parameters on UTS.

friction between two surfaces i.e. workpiece and the tool flatness and the pattern of the flow of the material in soft condition[32]. On the other hand, the WS decides the heat input to the process per unit length or per unit of the time to the workpiece. The TA causes the force applied behind the tool and also the flow of the material during the process[33,34]. So that the lower value of WS and higher value of RS caused high heat input to the welding zone which results in the grain growth in HAZ and lesser mechanical properties. Fig 2 (b) presents that the lower WS i.e. 35 mm/min and nominal RS i.e. 1500 RPM can fabricate an FSWed joint of higher strength. The interactional combination of these two parameters provides appropriate heat to the process which results in higher joint strength. The interactions of the RS and TA decide the flow pattern and axial force on the material in a soft condition which causes the proper mixing of the material during the welding process[35]. Figure 2 (c) shows that 1750 RPM and 3 degrees of RS and TA respectively, can provide the higher mechanical strength of FSWed joint. 2.5° of TA and 37.5 mm/min WS also results in the higher joint strength in their interactional effects as depicted in Fig. 2 (d).

3.3 Effects of process parameters on YTS:

It can be revealed from Table 7 (ANOVA Table for YTS) that all three parameters considered for variations are found significant for the variation of the output response i.e. YTS of the dissimilar FSWed joints. Figure 3 (a) presents the change that occurred in the values of the YTS with a change in the considered input parameters. The YTS starts increasing with the increment in the RS from 792 RPM to 1850 RPM and then it starts to decrease on further increment in RS. The almost same pattern can be seen while observing the effect of WS on the output YTS. The YTS seems to be increased when WS increases from 22 mm/min up to 35 mm/min but with the further increment in the WS it starts to fall. The value of YTS is increased with the increment of TA from 1° to 4° and then it starts decreasing with the further increment in the same as can be observed from Fig. 3 (a).

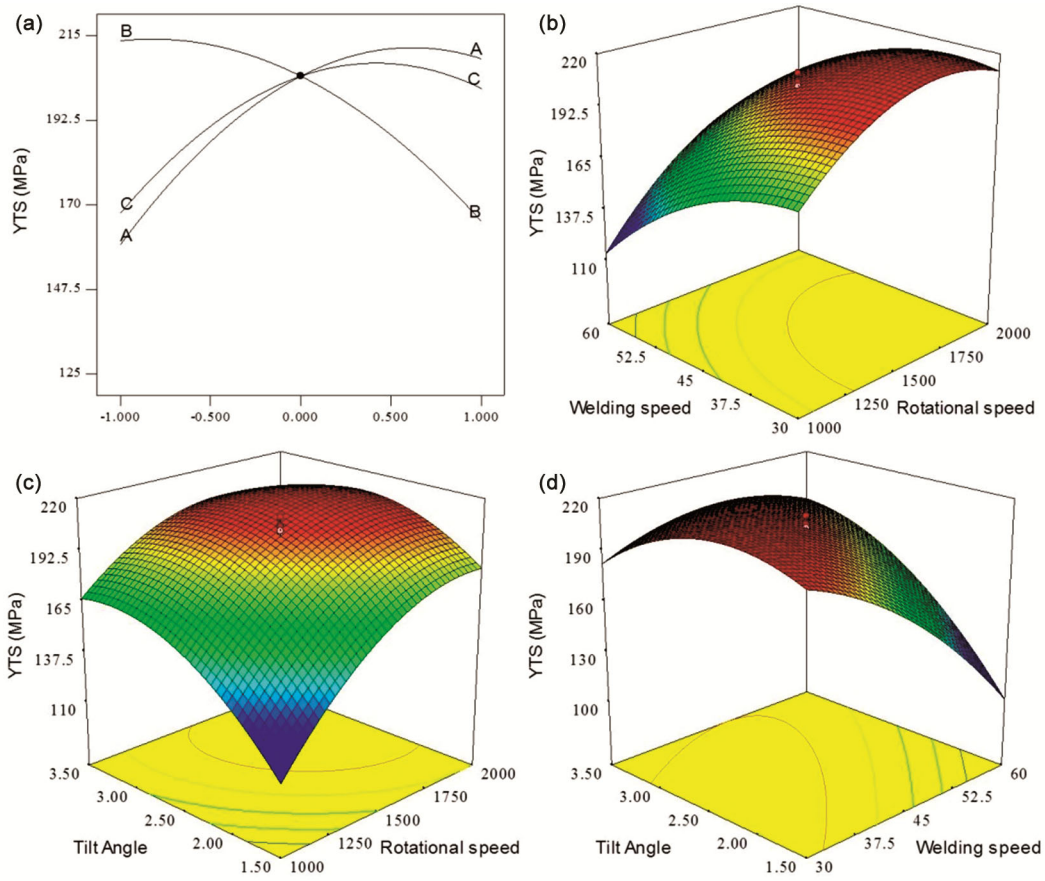

Fig. 3 — ANOVA plots for main and interactional effects of process parameters on YTS.

The output responses are affected by the variation of input parameters individually as well as their interactions with the other parameters. These interactional effects are the combined effects of the input parameters when changed simultaneously[36,37]. Table 6 shows that the interactions of RS with WS, RS with TA and WS with TA have significant effects on the variation of the considered response YTS. The results of these interactions on YTS are presented by 3D plots in Fig. 3.

The properties of FSWed joints are affected by the heat input and the flow of material during the welding process. The variation of input parameters is responsible for the above-said effects. The lower value of the RS causes the low heat frictional heat generation and higher WS causes the lower heat input to the material as well. This combination provides less heat to the material to be welded and this may cause improper softening and mixing of material in NZ [38]. The result of the discussed condition can be revealed from Fig. 3 (b) as it is presenting lower YTS at lower RS and higher WS but it is found higher with 1750 rpm RS and 37.5 mm/min WS, respectively. Where a higher value of RS is combined with the lower value of WS which provides proper heat to the welding process. TA decides the axial force and the direction of mixing of the material. YTS is observed higher at 3° TA and 1750 rpm RS as presented in Fig. 3 (c). WS can change the heat input to the welding process while the change in TA can change the axial force exerted and direction of the material mixing. Figure 3 (d) shows that YTS is found higher at a combination of 2.5° and 37.5 mm/min of TA and WS, respectively.

3.4 Effects of process parameters on EL

EL of the dissimilar FSWed joints of AA7039 and AA5083 are found significantly affected by the change in the considered input parameters as revealed in ANOVA results and presented in Table 8. Figure 4 presents the graphs of the pattern of changes in EL with the variation of the individual input parameters i.e. perturbation curves. EL of the tested joints is observed first increasing with the increment in RS

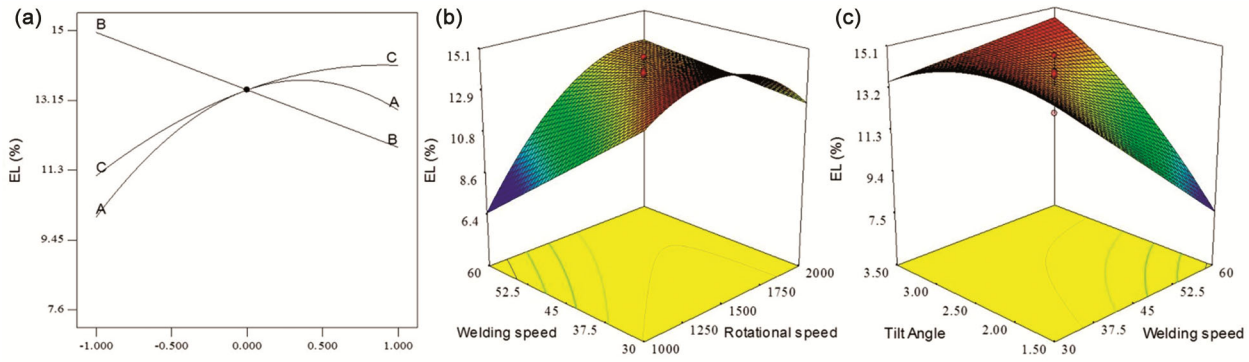

Fig. 4 — ANOVA plots for main and interactional effects of process parameters on EL.

Table 10 — Results of desirability test

S. No.	Rotating Speed(rpm)	Welding Speed (mm/min)	Tilt Angle (degree)	UTS (MPa)	YTS (MPa)	EL (MPa)	Desirability
1	1440.8	32.1	2.4	263.02	211.90	14.77	1
2	1584.0	30.3	2.0	265.14	217.73	14.84	1
3	1550.6	31.8	2.5	266.14	215.06	14.67	1
4	1445.3	32.4	2.3	263.28	212.12	14.73	1
5	1528.8	30.4	1.9	263.29	215.03	14.92	1
6	1452.1	31.7	2.4	263.39	212.37	14.81	1
7	1445.3	31.7	2.4	262.95	211.96	14.81	1
8	1583.6	30.6	2.4	266.72	216.82	14.75	1
9	1487.3	30.1	2.4	264.37	214.01	15.00	1
10	1548.5	30.8	2.6	263.77	212.95	14.68	1
11	1516.0	30.0	2.5	263.78	213.40	14.88	1
12	1618.9	30.0	2.3	266.81	218.47	14.76	1
13	1571.7	31.2	2.2	266.57	217.49	14.77	1
14	1574.1	30.2	2.3	266.62	217.32	14.86	1
15	1471.5	30.44	2.23	264.14	213.83	15.02	1
16	1754.5	50.36	3.25	271.66	206.88	14.66	0.98
17	1779.0	50.35	3.25	272.22	206.79	14.66	0.98

from 792 rpm to1600 rpm but it starts decreasing with a further increment of the same. The increment in WS from 24 mm/min up to 60 mm/min caused an increment in EL and then it has started to fall in EL with further increment. The continuous increase can be seen from the plot of the EL with the increment in TA from 1^{o} to 4^{o} in Fig. 4 (a).

The interactional effect of significant interactions i.e. RS with WS and WS with TA are presented with the help of 3D plots in Fig 4. The results of the 3D plots reveal that EL is found lower at a combination of higher WS and lower RS. The maximum EL can be attained with 1500 rpm and 30 mm/min RS and WS, respectively. EL is also at a lower level when WS is at a lower level and RS is at a higher level as depicted in Fig. 4 (b). As presented in Fig. 4 (c), The combination of higher WS and lower TA results in a low value of EL but it increases as a decrease in WS and increases in TA. EL can attain maximum value when TA and WS are maintained at 2.5^{o} and 30 mm/min, respectively.

3.5 Results of desirability (Multi-objective optimization):

Desirability function is the most widely used approach for multi-objective optimization in the industry for product design and process optimization. In this function, the score between 0 to 1 are assign to the individual response function, where 0 is not accepted and 1 is the most acceptable score. Table 10 presents the results of the desirability function approach, where top acceptable scores for multi-objective function are shown. The first 15 combinations of the input parameters can provide the sets of output responses for which the score of desirability function is 1 i.e. most acceptable.

Figure 5 presents the graphical representation of the first set or the most desirable set of combination of input parameters at which the values of output responses are highly acceptable. The figure reveals that RS, WS and TA at 1493.78 RPM, 30.35 mm/min and 2.6^{0}, respectively can provide the maximum possible values of UTS, YTS and EL i.e. 262.74 MPa, 212.21 MPa and 14.86 %, respectively.

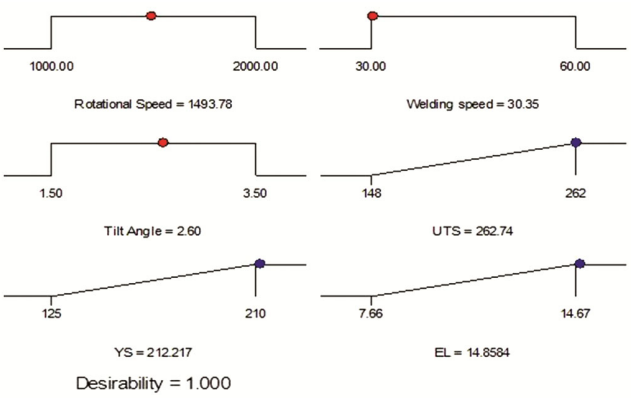

Fig. 5 — Graphical representation of Desirability results.

3.6 Microstructural analysis

The material to be welded during the FSW process requires the heat input and stiring action of the tool pin for welding. This heat input causes the alteration in the microstructure if the material. which results in the formation of NZ, TMAZ and HAZ as the zones in a welded section of the material[39,40]. The alteration in the microstructure of material causes changes in the properties of the FSWed joints. The overheat supply during FSW process causes unwanted and extra grain growth in HAZ of the joint. This results in loss of mechanical strength and hardness in this section. This type of joints breaks from the intersection of the TMAZ and HAZ. But the lower heat supply during the process may not be able to proper softening of the material. This results in the extra elongation in the TMAZ and this also results in a smaller TMAZ as well. This type of joints breaks from the intersection of NZ and TMAZ or from NZ itself[41,42]. So for the proper welding of the material, a proper amount of heat should be supplied to the process, which neither causes an extra grain growth in HAZ nor causes an extra elongation of grains in TMAZ[43,44].

To verify the changes in microstructure and their correlation with the mechanical properties of the joints some specimens are selected for microstructural analysis. The joints that showed the higher and the lower strength during the tensile tests are selected for this analysis. Figures 6 & 7 represent the effect of appropriate and a lower heat supply respectively, during FSW process and their effects on the welding of two different materials in dissimilar FSW, respectively. Lower heat supply during process caused improper mixing of the materials as presented in Fig. 7.

A proper or moderate heat generation and supply in FSW also result in the fine and equiaxed grains in NZ.

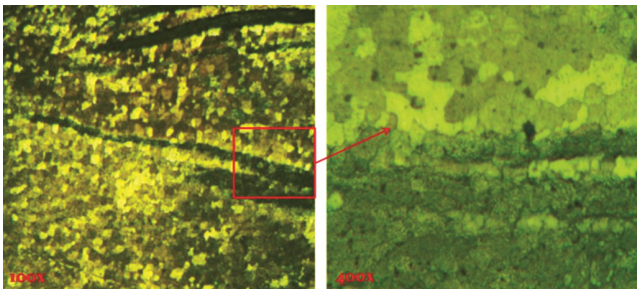

Fig. 6 — Bonding of dissimilar materials in NZ (sample 12).

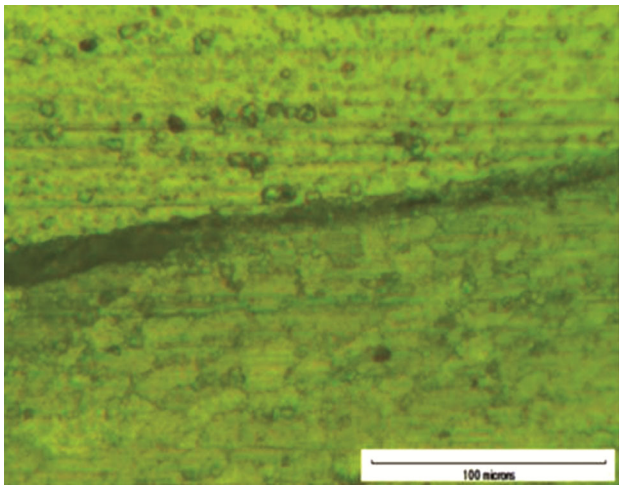

Fig. 7 — Presentation of bonding in NZ (sample 5.)

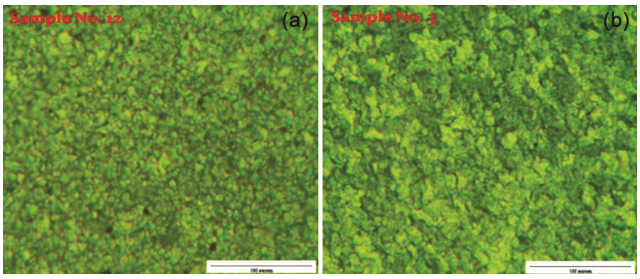

Fig. 8 — NZ of FSWed joints of Sample 12 and sample 3.

Figure 8 represents the above-said difference with the help of sample 12 and sample 3. Sample 12 shows the finer grains in NZ than sample 3 which is the result of variation in heat input during the welding process.

4 Conclusion

The present experimental study was an attempt to join the armor grad dissimilar alloys of aluminium by FSW. This attempt was performed to reveal the effects of process input parameters on the considered responses. The study also revealed the optimized set of these input parameters and the effects of variation

of these on the microstructure of FSWed joints. The present study outlined the following conclusions:

(a) All selected process parameters i.e. RS, WS and TA for the study, are found to have a significant contribution to the considered responses i.e. UTS, YTS and EL.
(b) The formulated mathematical models for all three responses are also found adequate in confirmatory test with 4.1%, 2.2% and 6.3% for UTS, YTS and EL respectively.
(c) Desirability test revealed the most desired set of optimized input parameters as 1440.8 RPM of tool rotational speed, 32.1 mm/min tool travels speed and 2.4 tool tilt angle, which can join dissimilar AA7039 and AA5083 with 263.02 MPa UTS, 211.90 MPa YTS and 14.77% EL.
(d) The microstructural analysis revealed that the change in values of responses with the variation of input parameters in due to a change in the microstructure of FSWed joins of AA7039 and AA5083.

References

1 Mishra R S, & Ma Z Y, *Mater Sci Eng,* 50 (2005) 1.
2 Thomas W M U, Nicholas E D, & Hall A, *Mater Des,* 18 (1998) 269.
3 DebRoy T, & Bhadeshia H K D H, *Sci Technol Weld Join,* 15 (2010) 266.
4 Cavaliere P, Cerri E, Marzoli L, & Dos Santos, J *Appl Compos Mater,* 11 (2004) 247.
5 Yan Y, Zhang D T, Qiu C, & Zhang W, *Trans Nonferrous Met Soc China (English Ed),* 20 (2010) 2.
6 Kundu J, Ghangas G, Rattan N, & Sharma S K, *Int J Curr Eng Technol,* 7 (2017) 1170.
7 Murr L E, *J Mater Eng Perform,* 19 (2010) 1071.
8 Park S W, Yoon T J, & Kang C Y, *J Mater Process Technol,* 241 (2017) 112.
9 Prasanth R S S, & Hans Raj K, *Trans Indian Inst Met,* 71 (2017) 453.
10 Sadeesh P, *et al., Procedia Eng,* 75 (2014) 145.
11 Ravikumar S, Rao V S, & Pranesh R V, *Proceedings of the World Congress on Engineering, I* (2013) 3.
12 Chen Y, Cao W, Li S, Chen C, & Xie, J *Transactions on Intelligent Welding Manufacturing*, 153 (2018)
13 Pabandi H K, Jashnani H R, & Paidar M, *J Manuf Process,* 31 (2018) 214.
14 Zhang C, Huang G, & Liu Q, *Mater Today Commun,* (2020) 101920.
15 Mohamed M, Ahmed Z, Ataya S, & Seleman M M E, *Metals (Basel),* 11 (2021) 181.
16 Ahmed M M Z, Jouini N, Alzahrani B, & Seleman M M E, *Metals (Basel)* 11, (2021) 1.
17 Ilangovan M, Boopathy S R, & Balasubramanian V, *Trans Nonferrous Met Soc China, (English Ed.*25 (2015) 1080.
18 Iyer R B, Dhabale R B, & Jatti V S, *IOP Conf Ser Mater Sci Eng,* (2016) 149.
19 Kundu J, & Singh H, *Eng Solid Mech,* 4 (2016) 125.
20 Jain S, Sharm N, & Gupta, R *Eng Solid Mech,* 6 (2018) 51.
21 Akinlabi E T, Dinaharan I, & Akinlabi S A, *Indian J Eng Mater Sci,* 24 (2017) 207.
22 Liu, X, Lan S, & Ni, J *Mater Des,* 59 (2014) 50.
23 Venkateswarlu D, Nageswara rao P, Mahapatra M M, Harsha S P, & Mandal N R, *J Mater Eng Perform,* 24 (2015) 4809.
24 Jamshidi Aval, H *Mater Des,* 87 (2015) 405.
25 Rodriguez R I, Jordon J B, Allison P G, Rushing T, & Garcia, L *Mater Des,* 83 (2015) 60.
26 Cavaliere P, De Santis A, Panella F, & Squillace, A *Mater Des,* 30 (2009) 609.
27 Khodir S A, & Shibayanagi, T *Mater Sci Eng B,* 148 (2008) 82.
28 Koilraj M, Sundareswaran V, Vijayan S, & Rao S R K, *Mater Des,* 42 (2012) 1.
29 *Stat-Ease Handbook for Experimenters*. www.statease.com.
30 Elsen S R, & Ramesh T, *Int J Refract Met Hard Mater,* 52 (2015) 159.
31 Khan N Z, Siddiquee A N, Khan Z A, & Mukhopadhyay A K *J, Alloys Compd,* 695 (2017) 2902.
32 Goyal A, & Garg R K, *Silicon* (2018) doi:10.1007/s12633-018-9858-4.
33 Pandey A K, Chatterjee S, & Siba Sankar Mahapatra, *Indian J Eng Mater Sci, 26* (2019) 298.
34 Ghangas G, & Singhal S, *Mater Res Express,* 6 (2019) 26553.
35 Goyal A, & Garg R K, *Sci Iran,* 26 (2019) 2407.
36 Emami S, Sadeghi-Kanani S, Saeid T, & Khan F, *Arch Civ Mech Eng,* 20 (2020) 1.
37 Goyal A, & Garg R K, *Int J Struct Integr,* 10 (2019) 162.
38 Goyal A, & Garg R K, *Mater Res Express,* 6 (2019) 56514.
39 Ghangas G, & Singhal, S *Mater Today Proc,* 5 (2018) 17107.
40 Wang Q, Zhao Z, Zhao Y, Yan K, & Zhang H, *JMADE,* 88 (2015) 1366.
41 Kundu J, & Singh H, *Eng Solid Mech,* 4 (2016) 125.
42 Shashi Kumar S, Murugan N, & Ramachandran, K K *Meas, J Int Meas Confed***,** 137 (2019) 257.
43 Ghangas G, & Singhal S, *Mater Res Express,* 5 (2018) 066555.
44 Sayer S, Yeni C, & Ertugrul O *Kov, Mater,* 49 (2011) 155.